Anal. Chem. **2005,** *77,* 5870−5876

Raman Spectroscopic Analysis of Biochemical Changes in Individual Triglyceride-Rich Lipoproteins in the Pre- and Postprandial State

J. W. Chan,*,†,‡ D. Motton,§ J. C. Rutledge,‡,§ N. L. Keim,|| and T. Huser†,‡

Lawrence Livermore National Laboratory, 7000 East Avenue, Livermore, California 94550, Department of Internal Medicine, School of Medicine, University of California, Davis, California 95616, NSF Center for Biophotonics Science and Technology, University of California, Davis, Sacramento, California 95817, and Western Human Nutrition Research Center, U.S. Department of Agriculture, Davis, California 95616

Individual triglyceride-rich lipoprotein (TGRL) particles derived from human volunteers are nondestructively analyzed by laser tweezers Raman microspectroscopy, and information on their composition and distribution is obtained. The Raman signature of single optically trapped very low-density lipoproteins (VLDL), a subclass of TGRL, which play an important role in cardiovascular disease, exhibits distinct peaks associated with molecular vibrations of fatty acids, proteins, lipids, and structural rearrangements of lipids. Our analysis of pre- and postprandial VLDL exhibits the signature of biochemical changes in individual lipoprotein particles following the consumption of meals. Interaction of VLDL with endothelium leads to the breakdown of complex triacylglycerols and the formation of a highly ordered core of free saturated fatty acids in the particle. A particle distribution analysis reveals trends in the degree to which this process has occurred in particles at different times during the postprandial period. Differences in particle distributions based on the different ratios of polyunsaturated to saturated fats in the consumed meals are also easily discerned. Individual lipoprotein particles hydrolyzed in vitro through addition of lipoprotein lipase (LpL) exhibit strikingly similar changes in their Raman spectra. These results demonstrate the feasibility of monitoring the dynamics of lipid metabolism of individual TGRL particles as they interact with LpL in the endothelial cell wall using Raman spectroscopy.

Lipoproteins are 10 nm−1 μm-diameter lipid particles found in blood that are responsible for the transport of fatty acids and cholesterol as fuel for cells throughout the body. Lipoproteins consist of a monolayer shell of phospholipids, cholesterol, and apoproteins enveloping a hydrophobic core of triglycerides and cholesterol esters.[1] Triglyceride-rich lipoproteins (TGRL) in blood are generated from an exogenous pathway (chylomicrons) and an endogenous pathway (very low-density lipoproteins; VLDL). Elevation of blood lipid levels after the consumption of a meal (postprandial hyperlipemia) is the result of contributions from both of these pathways. Once in the blood, postprandial lipoproteins are hydrolyzed by an enzyme anchored to endothelial cells, lipoprotein lipase (LpL), to form smaller remnant particles and other lipolysis products, such as free fatty acids. The composition and relative distribution of TGRL are implicated in the onset of atherosclerotic cardiovascular disease, the leading cause of morbidity and mortality in the United States and most of the Western world. These lipoprotein particles are known to penetrate the arterial wall and become trapped, initiating the early stages of atherosclerotic lesions. Therefore, acquiring information on the structure of lipoprotein particles in the pre- and postprandial states, as well as changes due to interactions with enzymes expressed on endothelial cells, will assist in elucidating the pathogenesis of atherosclerosis.

Previous studies using postprandial TGRL have primarily used standard ultracentrifugation and biochemical analysis techniques of bulk samples. These types of studies investigate entire populations of lipoproteins at a time and are therefore not specific to chemical differences between individual particles. Here, we demonstrate that a novel technique combining laser tweezers with confocal micro-Raman spectroscopy allows for the noninvasive, nondestructive analysis of individual TGRL in their native environment. Raman spectroscopy is a laser-based vibrational spectroscopy technique for the analysis of molecular bonds due to inelastic scattering of photons. Raman-scattered photons are scattered predominantly with a shift toward longer wavelengths (Stokes-shifted), whereby they deposit parts of their energy in the sample. The difference between the incident and scattered frequencies corresponds to the energy of the molecular vibration. Therefore, a Raman spectrum is a "molecular fingerprint" of the sample, providing a wealth of information about the chemical bonds associated with DNA, proteins, lipids, and carbohydrates commonly found in biological samples.[2] Changes in their composition thus reveal themselves as differences in the Raman spectrum. It has recently been shown that if Raman spectroscopy is combined with confocal microscopy, even individual cells or

* Corresponding author. E-mail: chan19@llnl.gov. Fax: (925) 424-2778.

† Lawrence Livermore National Laboratory.

‡ NSF Center for Biophotonics Science and Technology, University of California.

§ Department of Internal Medicine, University of California.

|| U.S. Department of Agriculture.

(1) Tulenko, T. N.; Sumner, A. E. *J. Nucl. Cardiol.* **2002**, *9*, 638−649.

(2) Peticolas, W. L. *Biochem. Spectrosc.* **1995**, *246*, 389−416.

10.1021/ac050692f CCC: $30.25
Published on Web 08/17/2005

subcellular components can be analyzed.[3] Femtoliter sample volumes can be analyzed with a diffraction-limited spatial resolution of better than 1 μm.

Individual biological samples in the nanometer-size regime that are unconstrained in their natural aqueous environment are usually difficult to probe by confocal Raman microspectroscopy. Typically, these particles need to be dried on the surface of a substrate, which may change their biological activity. Also, in this case, locating the nanometer-sized particles by scanning the substrate for Raman or fluorescence signals becomes extremely difficult, if not impossible, due to the background of the substrate and the minute particle size. By combining laser trapping with confocal Raman spectroscopy, such particles can be probed while naturally suspended in their native environment without the need for particle adhesion to a surface. Optical trapping in its simplest form involves the use of a single, tightly focused laser beam to immobilize a particle within the laser focus by optical forces.[4] Trapping is achieved as photons impinging on the particle transfer momentum from the light beam, imparting reaction forces on the object. The balance of both scattering and gradient forces on the object near the laser focus results in a stable three-dimensional optical trap. This technique, first pioneered by Ashkin and Chu,[5] has been used extensively in the biophysical sciences for the manipulation of biological samples (bacteria, viruses, cells, organelles)[6−9] and the determination of biomolecular interaction forces.[10,11] Recent work has applied laser tweezers Raman spectroscopy to the vibrational analysis of biological particles suspended in solution[12,13] Recently, Xie and co-workers,[14−16] for example, demonstrated the application of optical trapping combined with Raman spectroscopy and shifted excitation Raman spectroscopy to study the dynamics of thermal denaturation of *Escherichia coli* bacteria and yeast cells. Other recent work has also demonstrated the use of this method to analyze the composition and properties of individual liposomes.[17−19] This approach also allows for the determination of subpopulations in a mixed, heterogeneous sample,[12] an important parameter that cannot be obtained by conventional bulk spectroscopy.

The main goals of the present work are to determine to what level of detail information about the biochemical composition and biochemical changes can be extracted from single lipoproteins undergoing lipid metabolism. Such information can provide new insight into the chemical processes leading to atherosclerosis. In this study, a subgroup of TGRL particles, VLDL, are targeted for chemical analysis. Pre- and postprandial particles from human subjects consuming different diets are chemically characterized at different points in time during the postprandial state. We also determine biochemical changes in VLDL undergoing in situ hydrolysis during exposure to LpL and compare the results. In situ hydrolysis simulates the repeated lipolysis of lipoprotein particles by lipoprotein lipase anchored to the endothelial cell layer of blood vessels. To date, no studies have analyzed the composition and biochemical changes of *individual* plasma-derived lipoprotein particles undergoing lipoprotein metabolism and investigated the statistical variations in the composition from particle to particle. Few studies have been aimed at the Raman[20] or infrared (IR) spectroscopy[21,22] of lipoprotein structure, and they were all performed on bulk solutions of lipoproteins. Laser light scattering spectroscopy[23] has yielded bulk-averaged information about the size and density of lipoproteins before and after the onset of ischemia. Here, we show that the biomolecular Raman spectroscopic fingerprint of individual VLDL is unique, highly reproducible, and can be used to monitor biochemical changes of the particles due to lipoprotein metabolism.

EXPERIMENTAL SECTION

Preparation of TGRL Samples. Blood was obtained from human female volunteers participating in a clinical nutrition research study examining postprandial lipemia in response to meals with low and high glycemic loads. The study was approved by the Human Subjects Research Committee of the University of California, Davis, CA. All volunteers were overweight with BMI 27−29 and between 24 and 35 years of age. For 3 days prior to blood collection, volunteers consumed controlled diets with sufficient calories to match their individual energy requirements (2000−2200 kcal/d) and moderate fat content (30%). Fasting blood was obtained after a 12 h overnight fast. For the postprandial studies, volunteers consumed controlled mixed meals containing 30% total fat, 15% protein, and 55% carbohydrate. The mixed meal with the low glycemic load contained carbohydrates from whole grain products and a polyunsaturated/saturated (P/S) fat ratio of 0.2, whereas the high glycemic load meal contained carbohydrates from refined grain products and P/S ratio of 0.10. Postprandial blood was drawn at 3.5 and 8 h following meal ingestion. Blood was collected in 10 mL Vacutainer tubes filled with streptokinase (150 units/mL of blood). Whole blood was then spun at 4 °C for 10 min at 1750*g*, to remove cellular particulate. After centrifugation, plasma was transferred to ultracentrifuge tubes (Beckman-Coulter) and centrifuged at 285000*g* at 4 °C for 4 h to isolate TGRL. This procedure removes all higher density lipoprotein particles (LDL, HDL, and IDL) with a diameter of less than 40 nm. After ultracentrifugation, TGRL was removed and the concentration was measured using an Infinity Triglyceride Concentration kit (Sigma Diagnostics). The final samples containing only chylomicrons,

(3) Puppels, G. J.; Demul, F. F. M.; Otto, C.; Greve, J.; Robertnicoud, M.; Arndtjovin, D. J.; Jovin, T. M. *Nature* **1990**, *347*, 301−303.
(4) Molloy, J. E.; Padgett, M. J. *Contemp. Phys.* **2002**, *43*, 241−258.
(5) Ashkin, A.; Dziedzic, J. M.; Bjorkholm, J. E.; Chu, S. *Opt. Lett.* **1986**, *11*, 288−290.
(6) Block, S. M.; Blair, D. F.; Berg, H. C. *Nature* **1989**, *338*, 514−518.
(7) Ashkin, A.; Dziedzic, J. M. *Science* **1987**, *235*, 1517−1520.
(8) Ashkin, A.; Dziedzic, J. M.; Yamane, T. *Nature* **1987**, *330*, 769−771.
(9) Ashkin, A.; Dziedzic, J. M. *Proc. Natl. Acad. Sci. U.S.A.* **1989**, *86*, 7914−7918.
(10) Bustamante, C.; Bryant, Z.; Smith, S. B. *Nature* **2003**, *421*, 423−427.
(11) Visscher, K.; Schnitzer, M. J.; Block, S. M. *Nature* **1999**, *400*, 184−189.
(12) Chan, J. W.; Esposito, A. P.; Talley, C. E.; Hollars, C. W.; Lane, S. M.; Huser, T. *Anal. Chem.* **2004**, *76*, 599−603.
(13) Ajito, K.; Han, C. X.; Torimitsu, K. *Anal. Chem.* **2004**, *76*, 2506−2510.
(14) Xie, C. G.; Li, Y. Q.; Tang, W.; Newton, R. J. *J. Appl. Phys.* **2003**, *94*, 6138−6142.
(15) Xie, C. G.; Li, Y. Q. *J. Appl. Phys.* **2003**, *93*, 2982−2986.
(16) Xie, C. G.; Dinno, M. A.; Li, Y. Q. *Opt. Lett.* **2002**, *27*, 249−251.
(17) Cherney, D. P.; Bridges, T. E.; Harris, J. M. *Anal. Chem.* **2004**, *76*, 4920−4928.
(18) Cherney, D. P.; Conboy, J. C.; Harris, J. M. *Anal. Chem.* **2003**, *75*, 6621−6628.
(19) Sanderson, J. M.; Ward, A. D. *Chem. Commun.* **2004**, 1120−1121.
(20) Verma, S. P.; Philippot, J. R.; Bonnet, B.; Saintemarie, J.; Moschetto, Y.; Wallach, D. F. H. *Biochem. Biophys. Res. Commun.* **1984**, *122*, 867−875.
(21) Fraile, M. V.; Carmona, P. *Spectrochim. Acta Part A* **1996**, *52*, 557−563.
(22) Lopez, G.; Martinez, R.; Gallego, J.; Tarancon, M. J.; Carmona, P.; Fraile, M. V. *Appl, Spectrosc.* **2000**, *54*, 1771−1776.
(23) Vlasova, I. M.; Dolmatova, E. V.; Koshelev, V. B.; Saletsky, A. M. *Laser Phys. Lett.* **2004**, *1*, 417−420.

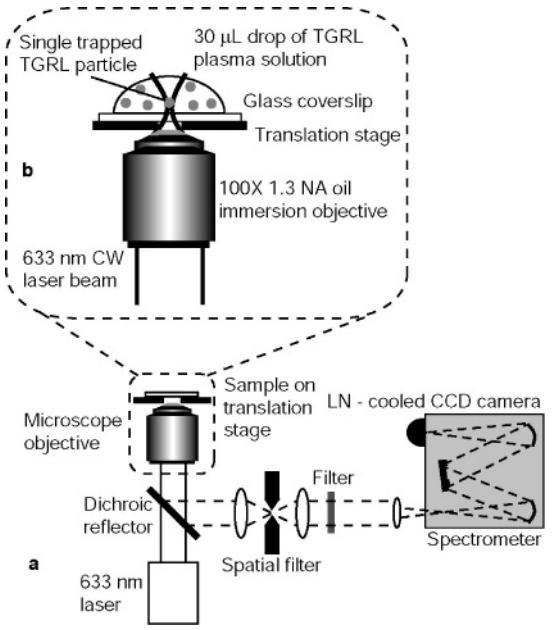

Figure 1. (a) Confocal spectroscopy system for the detection of the Raman spectra of single TGRL particles. (b) Optical trapping of a single TGRL particle in plasma solution and simultaneous spectral acquisition using a single laser beam focused through a high numerical aperture objective.

VLDLs and their remnants were stored on dry ice and then transported to LLNL. The plasma was diluted 1:100 in PBS buffer to separate and isolate individual TGRL in buffer solution. Analysis of the TGRL by LTRS was typically conducted no later than 48 h after extraction.

Acquisition of Raman Spectra of Single Optically Trapped TGRL. The LTRS system consists of a 632.8 nm CW laser beam spectrally filtered with a 633 nm band-pass filter and delivered into the back port of a Zeiss Axiovert 200 inverted microscope. A long-pass dichroic reflector directs the beam through a 100×, 1.3 NA oil immersion objective (Zeiss), resulting in a diffraction-limited spot of roughly 0.5 μm diameter with 10 mW laser power. The tight focus creates an optical trap that immbolizes single TGRL particles drifting in the plasma solution (Figure 1). White light illumination in transmission is used to obtain images captured on a CCD video camera. Epidetection of the Raman signals of the trapped particle is achieved using the same objective and a 100-μm pinhole in a confocal arrangement. The signals are filtered using a holographic 633 nm notch filter for suppression of residual laser light, directed into a spectrometer equipped with a 1200 lines/mm grating, blazed at 500 nm, and focused onto a liquid nitrogen-cooled CCD camera (1340 × 100 pixels). Optical trapping of single TGRL particles is accomplished by using the translation stage to move the particles to the proximity of the laser focus, at which point the particle will be drawn into the focus and then trapped. A typical acquisition time of 60 s is sufficient to acquire a Raman spectrum of typically better than 10:1 signal-to-noise ratio with clearly defined Raman bands. Spectra are calibrated to a toluene standard, and background correction is performed on each spectrum by subtraction of a third-order polynomial baseline fit. Each spectrum is normalized to the intensity of the 1440 cm^{-1} peak because fluctuations due to changes in protein concentration or conformation are relatively weak. The differentiation of the differently sized TGRL (large vs small) was based on their visibility in the optical microscope by comparison to polystyrene beads of well-known size.

Acquisition of Raman Spectra from Unsaturated and Saturated Oils. *cis*-9-Octadecenoic acid (oleic acid), hexadecanoic acid (palmitic acid), and octadecanoic acid (stearic acid) oil standards with purity greater than 95% were purchased from Sigma. The saturated fatty acid samples (palmitic acid and stearic acid are solid at room temperature. To simulate the effects of carbon chain disordering, samples of palmitic and stearic acid were also heated above their melting point in a water bath. The samples were examined at room temperature and ~70 °C, respectively, by placing either the powder (palmitic and stearic acids at room temperature) or liquid (oleic acid; palmitic and stearic acid heated above the melting point) on a calcium fluoride substrate. A 20× long working distance objective is used to focus the 633 nm laser beam onto the samples. Spectra are acquired with a 30 s integration time.

Hydrolyzation of TGRL Particles with Lipoprotein Lipase. LpL from bovine milk (diacylglycerol acylhydrolase) was purchased from Sigma. A 15-μL sample of the enzyme is added to ~1 mL of TGRL particles in plasma solution in an Eppendorf tube, with a density of 400 mg/dL. This results in a concentration of 1.4×10^{-2} mg/mL (74 total units) of enzymatic proteins. Spectra of many particles are taken both before and 60 min after addition of the LpL. Figure 5 shows a sample spectrum of individual particles before and after exposure to LpL and the background from LpL in buffer.

RESULTS AND DISCUSSION

In this study, we analyze the biochemical changes that occur in VLDL during normal human lipid metabolism. Even though the subject samples after ultracentrifugation also contain chylomicrons, those can be easily distinguished from VLDLs due to their significant difference in size. An initial calibration of our optical system using polystyrene beads of known sizes in solution revealed that only beads larger than ~150 nm can be visually observed using white light illumination in transmission and a 100 × 1.3 NA oil immersion objective. We use this value as a benchmark to discriminate between the "small" VLDL and remnant particles and "large" chylomicron particles in our samples that range in size typically from 40 to 1000 nm. We find that for, particles of roughly 150 nm and larger, a single trapped TGRL at the focus can be observed by white light imaging with a CCD camera (not shown). For smaller particles (<100 nm; VLDL and remnant particles), optical trapping is still feasible with the laser power used in this study. In this case, the TGRL are detected by the Rayleigh scattering of the laser light backscattered off the trapped particle (see the inset of Figure 2), which can be observed after removal of the filters in front of the CCD camera. It should be noted that for smaller particles it is possible that a cluster of particles is trapped at the laser focus rather than a single particle although this is minimized by appropriate dilution of the particle solution. Also, clustering in the case of polystyrene test particles led to fluctuations in the backscattered light intensity, which we did not observe in the case of TGRL. Therefore, we feel confident that we trapped individual TGRL for the duration of the Raman signal acquisition.

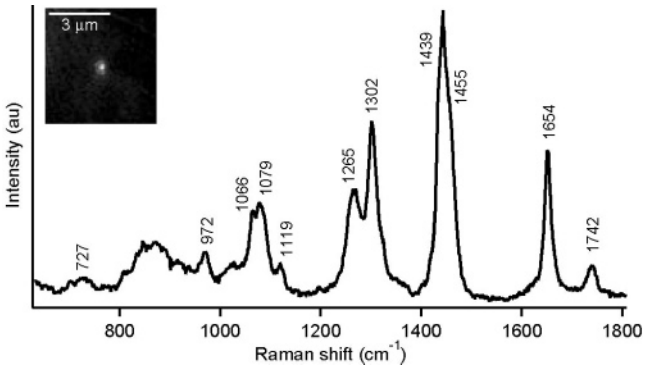

Figure 2. Raman spectrum of a single optically trapped TGRL particle taken with 10-mW laser power for 60 s (see table for peak assignments). A particle is confirmed to be trapped by detection of the backscattered laser light off the particle at the focus (see inset).

Table 1. Raman Frequencies of Individual TGRL and Their Assignments

Raman frequency in wavenumber units (cm^{-1})	assignment[a]
727	δ (=C−H) in-plane
972	δ (=C−H) out-of-plane
1066	ν(C−C)
1079	ν (C−C)
1119	ν (C−C)
1265	δ (=C−H) in-plane *cis*
1302	δ (CH_2) twisting
1439	δ (CH_2) scissor
1455	δ (CH_2)
1654	ν (C=C) cis (lipid), and ν (O−H) (water)
1742	ν (C=O) in $-CH_2-COOR$

[a] Abbreviations: ν and δ indicate stretching and deformation vibrations, respectively. See text for more details. Assignments are based on refs 24 and 25.

A typical background-corrected and normalized Raman spectrum of a single trapped TGRL particle is shown in Figure 2. This spectrum was obtained from a VLDL particle in plasma from a volunteer who consumed a controlled diet with moderate fat content (30%) for 3 days and then fasted for 12 h prior to sample extraction. We call this a 0-h sample, because it was obtained before the volunteers consumed a meal. The spectrum was obtained with a 60-s signal accumulation time using 10 mW of 633-nm laser power and shows a rich vibrational structure. The major peaks and their assignments are listed in Table 1.

The peaks observed in this 0-h spectrum of a VLDL particle can be readily assigned to known major lipid bands by comparing them to previously published results. Frank et al.[24] have observed similar Raman bands in human breast tissue and studies on oils and fats have also observed similar spectra.[25,26] The peak at 727 cm^{-1} is assigned to an in-plane bending mode of the C−H bond in a double bond. The 972-cm^{-1} peak is an out-of-plane deformation mode of the C−H bond. The peaks at 1066, 1076, and 1129 cm^{-1} correspond to C−C stretching vibrations, and the 1266-cm^{-1} peak is due to an in-plane C−H bending mode in a double bond. The peak at 1302 cm^{-1} can be attributed to a CH_2 twisting mode, the 1439-cm^{-1} peak to a CH_2 scissor mode, the 1654 cm^{-1} peak to a C=C stretch mode (indicative of unsaturated bonds), and the 1742-cm^{-1} peak to a C=O bond in an ester. The broad shoulder on both sides of the 1654-cm^{-1} band is a background contribution from the O−H stretching vibration of water in the plasma solution. These peaks provide information about the chemical components and conformations of the VLDL. It is known[25] that spectra of triacylglycerol exhibit the presence of the 1742-cm^{-1} peak that is lacking in spectra of free fatty acids, confirming that triacylglycerol is likely present in the core of the lipoprotein particle. The location of the 1650-cm^{-1} band indicates a cis conformation in the C=C double bond, which would otherwise be located at 1668 cm^{-1} for the trans conformation, and is therefore another marker for unsaturated bonds. The presence of the 1266-cm^{-1} band also indicates a cis geometry. Raman bands due to apoprotein modes, however, are difficult to identify because of the overwhelming contributions from lipids. For example, the amide I band at 1655 cm^{-1} is not easily distinguished from the 1655-cm^{-1} lipid band and the broad water background band. It is also difficult to isolate spectral signatures directly assignable to triglycerides and fatty acids in the core of the particles from the signals that are due to the phospholipid outer shell.

To aid in the characterization of Raman spectroscopic differences between VLDLs extracted at different points in time, Raman signatures of various oil standards were acquired. Figure 3 shows the Raman spectra of three different types of fatty acids. *cis*-9-Octadecenoic acid is a monounsaturated fatty acid with an 18-carbon atom chain with one double bond in the cis configuration. Hexadecanoic and octadecanoic acids are both saturated fatty acids with 16- and 18-carbon atom chains, respectively. The Raman spectra of the saturated fatty acids at room temperature are noticeably different from that of the unsaturated fatty acid. Very distinct, narrow sharp peaks at 891, 1062, 1097, 1128, 1296, 1419, and 1440 cm^{-1} are observed in addition to the absence of peaks at 1266 and 1655 cm^{-1}. These characteristic peaks have been previously observed[25] and identified in saturated triacylglycerols and saturated free fatty acids probed by Fourier transform Raman spectroscopy. The peaks, specifically at 1062, 1097, and 1128 cm^{-1}, can be assigned to C−C stretching in a hydrocarbon chain and the 1296-cm^{-1} peak to a CH_2 twist. The intensity and relative positions of the peaks in the 1000−1150-cm^{-1} region are sensitive to the conformational state of the hydrocarbon chain. The 1062- and 1128-cm^{-1} vibrations have been assigned to highly ordered all-trans chain segments while the 1097-cm^{-1} vibration is associated with structures having gauche rotations.[18,27−29] A highly disordered chain results in a broadening of the gauche band and shifts to lower frequency in addition to decreases in intensity of both the 1128- and 1063-cm^{-1} bands. Therefore, the Raman spectra of palmitic and stearic acids at room temperature indicate that these fully saturated hydrocarbon chains are highly ordered while oleic acid, an unsaturated fatty acid with a carbon−carbon double bond, results in chain disorder. If palmitic and stearic acids are

(24) Frank, C. J.; Redd, D. C. B.; Gansler, T. S.; Mccreery, R. L. *Anal. Chem.* **1994**, *66*, 319−326.
(25) Weng, Y. M.; Weng, R. H.; Tzeng, C. Y.; Chen, W. L. *Appl, Spectrosc.* **2003**, *57*, 413−418.
(26) Baeten, V.; Hourant, P.; Morales, M. T.; Aparicio, R. *J. Agric. Food Chem.* **1998**, *46*, 2638−2646.
(27) Brown, K. G.; Peticolas, W. L.; Brown, E. *Biochem. Biophys. Res. Commun.* **1973**, *54*, 358−364.
(28) Spiker, R. C.; Levin, I. W. *Biochim. Biophys. Acta* **1975**, *388*, 361−373.
(29) Gaber, B. P.; Peticolas, W. L. *Biochim. Biophys. Acta* **1977**, *465*, 260−274.

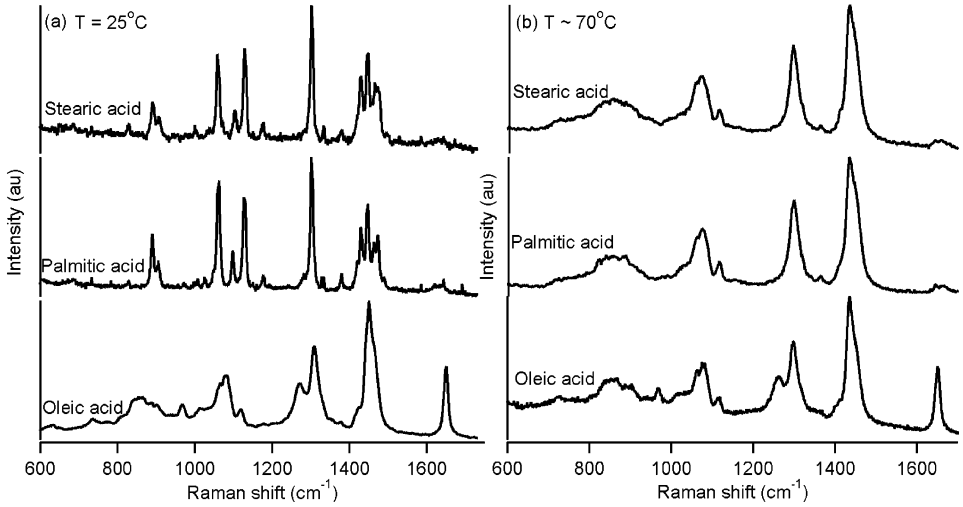

Figure 3. Raman spectra of oleic, palmitic, and stearic acid at (a) room temperature and (b) 70 °C. Saturated fatty acids (palmitic and stearic acids) at room temperature exhibit a number of unique sharp spectral peaks, e.g., at 1062, 1128, and 1296 cm^{-1}, that are not observed for the unsaturated oleic acids. These changes indicate highly ordered carbon chains in the saturated fatty acids, which disappear at temperatures above the melting point (b). In this case, the C═C vibrations at 1266 and 1655 cm^{-1} become the most distinct differences between the fatty acid standards.

heated above their melting point to induce disorder in the hydrocarbon chains, the sharp peaks that are assigned to highly ordered chains disappear and the spectra become more like that of oleic acid. Peaks due to unsaturated double bonds at 1266 and 1655 cm^{-1}, however, are not present. We can thus use the presence of sharp peaks in the 1000−1150 cm^{-1} range as markers for highly ordered saturated fatty acids, whereas peaks at 1266 and 1655 cm^{-1} indicate the presence of unsaturated fatty acids.

We have obtained Raman spectra of individual VLDLs obtained from volunteers at 0, 3, and 8 h, respectively, after consumption of high and low glycemic load test meals. Between 20 and 30 VLDL particles were examined at each time point. All subjects were held on either high or low glycemic diets, which had been consumed for 3 days prior to the test meal. Figure 4 shows the average Raman spectra of the particles from the three time intervals for both high and low glycemic load diets. Also shown are the 3- and 8-h difference spectra after subtraction of the 0-h spectra. The spectra clearly reveal differences in the Raman spectra at 3 and 8 h after meal ingestion. Most notable are the formation of distinct, sharp peaks at 1060 and 1129 cm^{-1}, a decrease in the 1266 cm^{-1} band, a shift and narrowing of the peak at 1298 cm^{-1}, an increase in the 1099 cm^{-1} peak intensity, and a decrease in the 1650 cm^{-1} band for both test subjects.

Note that the 0 h spectra for both volunteers are very similar to those obtained from the unsaturated oleic acid. This indicates that these VLDLs are highly unsaturated and have a relative lack of any saturated fatty acids in the core of the particle. The peaks in these Raman spectra are mainly due to vibrational signatures of the phospholipid shell in addition to cholesterol ester and unsaturated fatty acids in the particle. The results from our pre- and 3 and 8 h postprandial study of biochemical changes in VLDL particles (Figure 4) indicate that, following meal consumption, the main biochemical changes in VLDLs are that the long hydrocarbon lipid chains in the particle adopt a higher ordered conformation, based on the observed changes in the 1000−1150 cm^{-1} region. Also, peaks due to unsaturated bonds (e.g., 1265 and 1654 cm^{-1} peaks associated with C═C bonds) are decreasing in intensity for the postprandial particles.

These spectral changes reveal detailed information on the biochemical changes that are occurring in the particles as VLDL is hydrolyzed through repeated exposure to LpL on endothelial cell membranes. The triacylglycerols initially present in the particle are complex molecules, where the three hydrocarbon chains may consist of combinations of very different fatty acid chains (e.g., saturated and unsaturated chains, long and short chains, and unsaturated chains with double bonds in different positions). Since it is known that saturated and unsaturated chains do not preferentially mix, instead favoring the formation of separate domains, triacylglycerol molecules encounter steric problems because the covalently linked fatty acid chains are forced to pack together. Therefore, these molecules adopt highly disordered packing.[30−34] Following meal consumption, the triacylglycerol molecules packed in the particle core undergo hydrolysis as the particle interacts with endothelium and are broken down to form unsaturated and saturated free fatty acids, which are now free to form separate highly ordered domains. Accordingly, increases in the peaks in the 1000−1150 cm^{-1} spectral region indicate the presence of highly ordered cores of saturated fatty acids only in the 3 and 8 h postprandial particles.

One of the main benefits of laser tweezers Raman spectroscopy is that it enables the analysis of individual particles and their statistical distributions. We can use this technique to determine particle distributions based on variations in the chemical composition from particle to particle of the same type. Here, the relative distribution of fatty acids in particles in the 3 and 8 h postprandial states is used to assess differences in VLDL lipolysis depending on the fat content of a meal. The normalized value of the 1060 cm^{-1} Raman peak from individual particle spectra was used as a

(30) Kaneko, F.; Yano, J.; Sato, K. *Curr. Opin. Struct. Biol.* **1998**, *8*, 417−425.
(31) Small, D. M. *J. Lipid Res.* **1984**, *25*, 1490−1500.
(32) Di, L.; Small, D. M. *J. Lipid Res.* **1993**, *34*, 1611−1623.
(33) Di, L.; Small, D. M. *Biochemistry* **1995**, *34*, 16672−16677.
(34) Small, D. M. *Curr. Opin. Struct. Biol.* **1998**, *8*, 413−416.

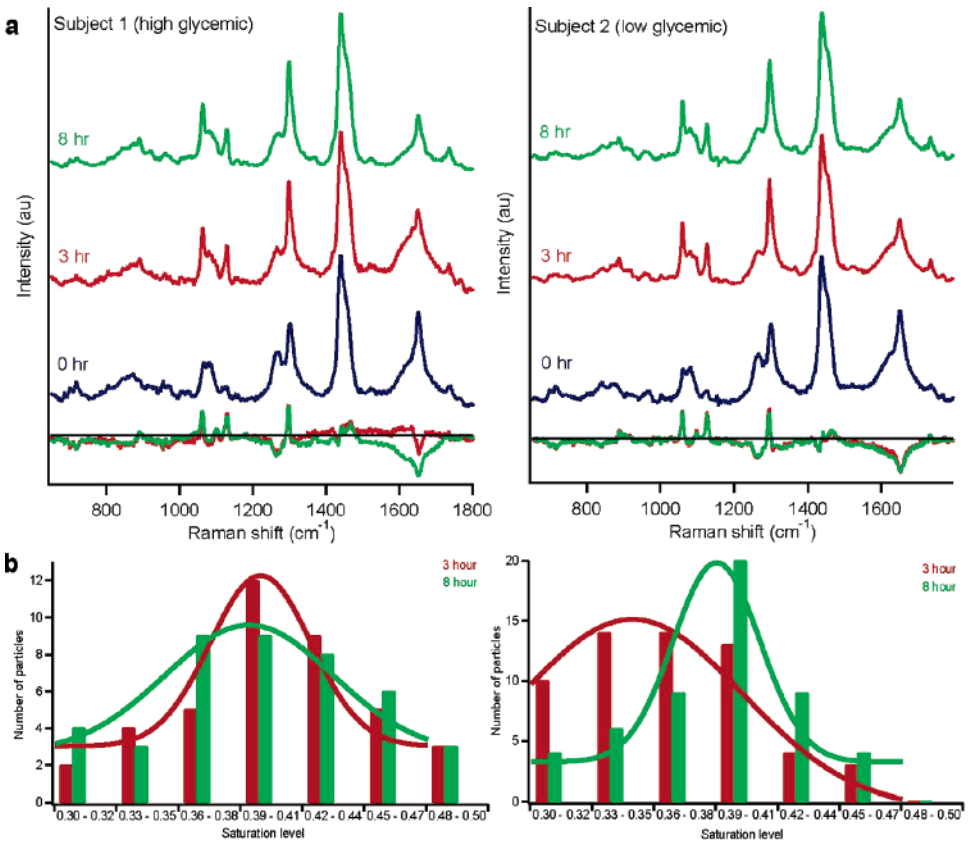

Figure 4. (a) Averaged Raman spectra of TGRL particles extracted from human volunteers at three time intervals before and after the consumption of a meal, and the 3 and 8 h difference spectra. (b) Plots showing the particle distribution based on the intensity of the 1060-cm^{-1} peak, indicative of the concentration of highly ordered saturated fatty acids in the particles. Solid lines are fits to the particle distributions and serve only as guides to the eye.

marker associated with high levels of highly ordered hydrocarbon chains, which represent saturated fatty acids at room temperature. Figure 4b shows a distribution plot of the saturation levels (i.e., peak intensity) of particles at 3 and 8 h for both diets. The distribution plots clearly show that the saturation levels from particle to particle vary greatly for both the low and high glycemic load meals and at different times in the postprandial period. The 3 h postprandial particles from the low glycemic study appear to have an overall higher degree of unsaturation compared to those from the high index study. This distribution shifts to the right at 8 h, indicating a lipolysis-related increase in free saturated fatty acids with time during the postprandial state. In contrast, the particles from the high glycemic study have a similar broad distribution at both times with no significant change in the peak position between 3 and 8 h postprandial time. One of the main differences between the two meal types is the total saturated fat content of the low and high glycemic load test meal (16.2 and 17.1 g, respectively). It appears that the distribution analysis of the 3 h postprandial particles directly reflects the content of saturated fatty acids of the ingested meal, while the 8 h postprandial particle spectra no longer reflect the saturation level of the meals. For a meal with higher content of saturated fatty acids, postprandial VLDLs contain higher amounts of saturated triacylglycerols that apparently require repeated exposure to LpL to convert them to free saturated fatty acids, which can then be detected spectroscopically. We believe that the reason for this observed behavior is that most of the triglycerides in the 3 h TGRL particles still originate exogenously (i.e., from the meal) while at 8 h, most of the triglycerides in the particles are the result of secondary liver metabolism and not remnants of exogenous triglycerides. Therefore, it is likely that the saturated triglycerides that we observe in the 8 h spectra represent the result of liver metabolism, containing bound fatty acids representative of de novo lipogenesis. Note the marked difference between the 8 h spectra and the 0 h spectra. The 0 h spectra were obtained after a 12 h fasting period. This indicates that the highly ordered saturated fatty acids found in VLDLs 8 h after meal consumption are removed and converted some time between the 8 and 12 h time frame. This process could be related to the transfer of fatty acids or triacylglyerols to other lipoprotein particles via transfer proteins. These plots demonstrate the ability of this technique to detect subtle changes and subdistributions in the composition of single particles that bulk or averaged spectral analysis cannot offer. However, additional experiments encompassing a larger set of data from many subjects are still required to draw definitive conclusions about these observed trends.

To further elucidate the effect of LpL hydrolysis on individual VLDL particles, we exposed TGRL particles to LpL, an enzyme found anchored to the endothelial cell surface. Normalized Raman spectra of individual lipoprotein particles before and after exposure to LpL are shown in Figure 5. We observe a slight decrease in the 1742 cm^{-1} peak following hydrolysis, indicating that the triglycerides are being converted to free fatty acids. Most notable are the formation of narrow peaks at 1060, 1097, 1129, and 1298

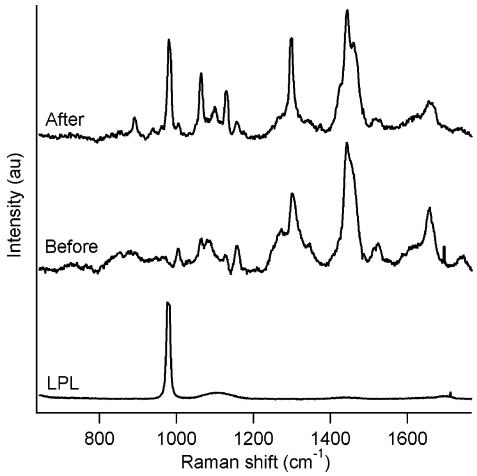

Figure 5. Individual Raman spectra of TGRL particles before and after 1 h exposure to lipoprotein lipase. The Raman spectrum of lipoprotein lipase is also shown.

cm^{-1} and a decrease in the 1265 and 1655 cm^{-1} peaks. Since there is no pathway for the addition of saturated fatty acids during this experiment, these spectral changes are clearly not a result of increased amounts of saturated oils in the particle but rather a direct indication of the enzymatic reaction occurring between the VLDL particle and the LpL enzyme, as discussed above. These changes indicate that, after hydrolysis of the triacylglycerol-containing particles, the saturated fatty acids are free to form separate domains, resulting in a particle that now consists of a core with highly ordered chains. This result is very similar to the biochemical changes observed in the postprandial particles extracted after different periods in time and confirms that we are observing biochemical changes in the native VLDL particles that are due to repeated exposure to LpL.

CONCLUSIONS

We have, for the first time, demonstrated that individual lipoproteins can be isolated, visualized, chemically characterized, and analyzed in an entirely noninvasive fashion. Previous studies have mainly analyzed ensembles of lipoproteins. Moreover, our ex vivo analysis of individual lipoproteins can be performed rapidly and at near-physiological conditions (TGRL in pure plasma and PBS solution). This obviates the need for long, complicated, and potentially destructive lipoprotein preparation protocols. This study has shown that, in the population of TGRL that we analyzed by LTRS, triacylglycerols are hydrolyzed by repeated exposure to LpL, resulting in free fatty acids. The free unsaturated and saturated fatty acids can pack into different phases, leading to the formation of a highly ordered saturated core, which can be detected spectroscopically. The particle distribution plots based on the level of highly ordered saturated fatty acids show that at the peak of the postprandial period (3 h after consumption of a meal) a correlation can be made between the P/S ratio of an ingested meal and the degree of saturation of the postprandial particles using the LTRS method. This result is not obvious from the averaged particle spectra shown in Figure 3a. These results demonstrate the benefits of this single-particle technique over bulk spectroscopy methods, which average over millions of particles. We expect that the combination of laser tweezers with Raman spectroscopy will ultimately allow us to follow the changes in chemical composition of a single TGRL as it is hydrolyzed by lipoprotein lipase on the endothelial cell membrane. Interactions of TGRL with endothelium can be facilitated by optically suspending the particle above a layer of endothelial cells for the Raman investigation and then deliberately initiating contact of the TGRL with the endothelial cell layer and continuing spectral interrogation during its interaction with endothelium and lipolysis by lipoprotein lipase. In addition, compositional changes in a single TGRL particle can be monitored as it is exposed to lipoprotein lipase, saturated fatty acids, and other lipids or proteins added to the buffer containing TGRL. There is considerable interest in understanding the different fatty acid conformations, complex chain-ordering effects, and packing, especially as it pertains to interactions within biological membranes and membrane rafts. Here, we have demonstrated such a study on chain reordering and interactions in a natural biological sample using LTRS.

ACKNOWLEDGMENT

This work was supported by the Richard A. and Nora Eccles Harrison Endowed Chair in Diabetes Research, National Institutes of Health under Grants HL55667 and HL71488. D.M. is supported by a supplement to HL71488. The clinical trial was supported by funds from the U.S. Department of Agriculture, Agricultural Research Service, CRIS5330-510000-002-00D. Funding for this work at Lawrence Livermore National Laboratory was provided by the Laboratory Directed Research and Development Program. This work was also supported by funding from the National Science Foundation. The Center for Biophotonics, an NSF Science and Technology Center, is managed by the University of California, Davis, under Cooperative Agreement PHY 0120999. Work at LLNL was performed under the auspices of the U.S. Department of Energy by the University of California, Lawrence Livermore National Laboratory, under Contract W-7405-Eng-48.

Received for review April 21, 2005. Accepted July 4, 2005.

AC050692F